

## Crystal Structure of Epstein-Barr Virus Protein BCRF1, a Homolog of Cellular Interleukin-10

Alexander Zdanov<sup>1</sup>, Céline Schalk-Hihi<sup>1</sup>, Satish Menon<sup>2</sup>  
Kevin W. Moore<sup>2</sup> and Alexander Wlodawer<sup>1\*</sup>

<sup>1</sup>Macromolecular Structure Laboratory, NCI-Frederick Cancer Research and Development Center, ABL-Basic Research Program  
Frederick, MD, 21702, USA

<sup>2</sup>Department of Molecular Biology, DNAX Research Institute, Palo Alto  
CA 94304, USA

The crystal structure of Epstein-Barr virus protein BCRF1, an analog of cellular interleukin-10 (IL-10), has been determined at the resolution of 1.9 Å and refined to an *R*-factor 0.191. The structure of this cytokine is similar to that of human IL-10 (hIL-10), forming an intercalated dimer of two 17 kDa polypeptides related by a crystallographic 2-fold symmetry axis. BCRF1 exhibits novel conformations of the N-terminal coil and of the loop between helices A and B compared to hIL-10. These regions are likely to be involved in binding of one or more components of the IL-10 receptor system, and thus the structural differences may account for the lower binding affinity and limited spectrum of biological activities of viral IL-10, compared to hIL-10.

© 1997 Academic Press Limited

**Keywords:** cytokines; interleukins; receptor binding; crystal structure; viral proteins

\*Corresponding author

### Introduction

Interleukin-10 (IL-10) is a helical cytokine produced by activated T cells, B cells, monocytes/macrophages, mast cells, and keratinocytes. IL-10 regulates several important aspects of the immune response, by suppressing activation of macrophages, inhibiting their ability to produce other cytokines and to serve as accessory cells for stimulation of T cell and natural killer cell function. For that reason, IL-10 was originally called a cytokine synthesis inhibitory factor (CSIF) (Fiorentino *et al.*, 1989; Moore *et al.*, 1990). IL-10 also plays a role in stimulating proliferation and differentiation of B cells, mast cells, and T cells (Ho & Moore, 1994). It has been shown recently that some viruses appear to make use of IL-10 function to inhibit expression of a variety of cytokines that regulate an effective immune response. Epstein-Barr virus (EBV) and equine herpesvirus type 2 encode viral homologs of IL-10 (Moore *et al.*, 1990; Vieira *et al.*, 1991; Rode *et al.*, 1993), while respiratory syncytial virus (RSV) induces RSV-infected alveolar macrophage production of host IL-10 (Panuska *et al.*, 1995). In either case, the resulting effect appears to be the suppression of the production of early immunoregulatory cytokines, leading to ineffective immune response.

While a number of structures of helical cytokines have been determined in the last decade by X-ray crystallography and NMR spectroscopy (reviewed by Davies & Wlodawer, 1995), all of them were recombinant versions of the mammalian proteins. Viral homologs of such cytokines have never been studied previously. We have now determined the crystal structure of BCRF1, the EBV homolog of IL-10, also known as viral IL-10 (vIL-10). This virally produced cytokine exhibits many activities of hIL-10 including its ability to inhibit production of other cytokines, but is significantly impaired in its binding to the IL-10 receptor (IL-10R; Ho *et al.*, 1993; Liu *et al.*, 1994). vIL-10 is a 17 kDa protein having 85% amino acid sequence identity with hIL-10. Fourteen out of 15 deletions, as well as four out of 13 substitutions, are found in the N terminus of vIL-10 (Figure 1), indicating that with the exception of 20 N-terminal residues, the rest of the structure of vIL-10 has to be very similar to that of hIL-10. However, functional differences between human and viral IL-10, such as ~1000-fold lower binding affinity of vIL-10 for recombinant hIL-10R and the fact that vIL-10 possesses only a subset of the activities of the hIL-10 (Liu *et al.*, 1997), imply that in spite of a high degree of sequence similarity there must be structural differences between these two proteins. Here, we report the structure of vIL-10 refined at 1.9 Å resolution, and compare it with the structures of hIL-10, previously solved in two crystal forms at 1.8 Å (Zdanov *et al.*, 1995), 1.6 Å

Abbreviations used: IL-10, interleukin-10; hIL-10, human IL-10; vIL-10, viral IL-10; IL-10R, IL-10 receptor.

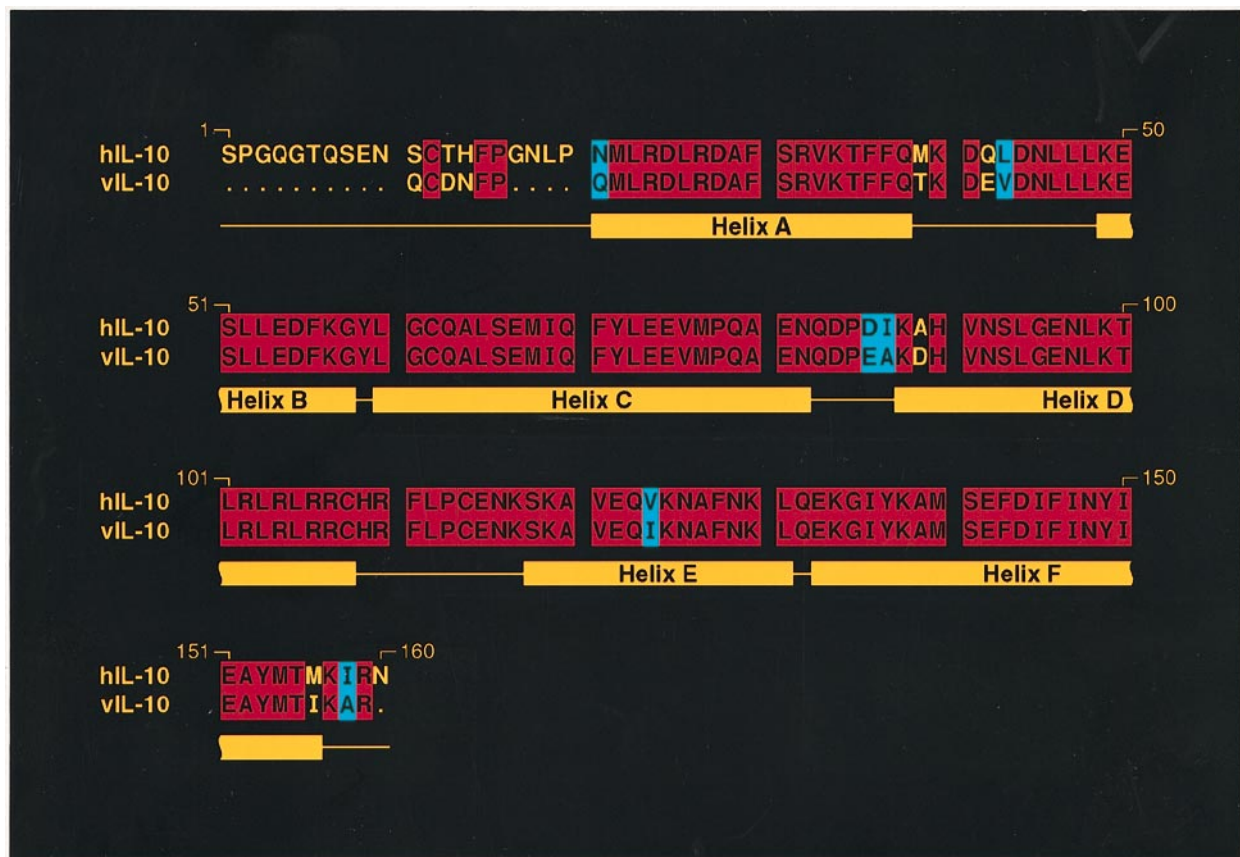


**Figure 1.** The alignment of amino acid sequences of viral and human IL-10. Identical residues are shown in red, similar residues in blue.

(Zdanov *et al.*, 1996), and 2.0 Å resolution (Walter & Nagabhushan, 1995).

## Results

### Solution and quality of the structure

We have obtained tetragonal crystals of vIL-10 diffracting up to the resolution of 1.9 Å, which proved to be isomorphous to the previously reported tetragonal crystal form of hIL-10 (Table 1). However, since these coordinates (Walter & Nagabhushan, 1995) had not yet been released at that time, the structure was solved by the molecular replacement method, using the high resolution structure of hIL-10 in the trigonal crystal form (Zdanov *et al.*, 1996) as a starting model. In contrast to the structure of hIL-10 in the tetragonal crystal form, where residues 1 to 17, 38 to 44, 108 to 110, and 160, including the disulfide bridge Cys12–Cys108, are disordered (Walter & Nagabhushan, 1995), the main-chain of vIL-10 could be traced almost in full (Table 1). Only one N-terminal and two C-terminal residues could not be located, although the regions, which are disordered in the tetragonal hIL-10, also have a much higher degree of flexibility than the rest of the molecule of vIL-10. The *R*-factor for the final model, which includes 142 out of 145 residues and 75 water molecules, is 0.191 for the 10 to 1.9 Å resolu-

tion shell. The root-mean-square (rms) deviation of the bond lengths from their target values is 0.019 Å, the angle distances deviate by 0.049 Å and the rms deviation from planarity is 0.018 Å.

### An overall structure of vIL-10

A molecule of vIL-10 is a homodimer consisting of two domains (Figure 2(a)). Each monomer contains six helices (A to F), four contributing to the formation of one of the domains and two to the other. Helices A, C, D, and F' form a classical left-handed four-helix bundle (Presnell & Cohen, 1989), found in all crystal structures of helical cytokines. Helices A to D of each monomer form a rigid frame with a highly hydrophobic depression in its middle. Helix F' of the symmetry-related monomer penetrates through the loop AB and covers this depression from the top, while helix E' covers it at the bottom, forming two structural domains with an extensive buried hydrophobic core.

As expected on the basis of the high degree of sequence similarity the tertiary structure of vIL-10 is very close to that of hIL-10, although the V-shaped dimer of both vIL-10 and tetragonal hIL-10 is slightly more "open" than that of trigonal hIL-10, with the elbow angle between its domains about 2° larger (Figure 2(b)). This phenomenon is reminiscent of the structures of antigen-binding fragments (Fab) of antibodies, where elbow angles

**Table 1.** Crystallographic data for the structures of IL-10 that have been determined to date

	hIL-10 NCI-FCRDC	hIL-10 NCI-FCRDC	hIL-10 Univ. of Alabama	vIL-10 NCI-FCRDC
<i>a</i> (Å)	70.27	69.53	36.56	36.27
<i>b</i> (Å)	70.27	69.53	36.56	36.27
<i>c</i> (Å)	70.31	70.54	220.97	219.60
$\alpha$ (deg.)	90	90	90	90
$\beta$ (deg.)	90	90	90	90
$\gamma$ (deg.)	120	120	90	90
Space group	P3 <sub>2</sub> 21	P3 <sub>2</sub> 21	P4 <sub>3</sub> 2 <sub>1</sub> 2	P4 <sub>3</sub> 2 <sub>1</sub> 2
Resolution (Å)	1.8	1.6	2.0	1.9
<i>R</i> (%)*	15.6	16.3	22.1	19.1
Disordered residues (hIL-10 numbering)	1-9	1-5	1-17, 38-44, 108-110, 160	11, 158-159

\* $R = \sum |F_{\text{obs}} - F_{\text{calc}}| / \sum F_{\text{obs}}$ , where  $F_{\text{obs}}$  and  $F_{\text{calc}}$  are observed and calculated structure factor amplitudes, respectively.

between variable and constant domains can change easily depending upon different crystal packing (Davies & Chacko, 1993). The rms deviation between the positions of C $\alpha$  atoms of one domain of vIL-10 *versus* trigonal and tetragonal hIL-10 are 0.65 Å and 0.46 Å, respectively. While the conformation and the arrangement of the helices in the corresponding domains of vIL-10 and hIL-10 are quite conserved, those of the loops are different. Three such loops are present in the IL-10 molecule, joining helices A and B (loop AB), C and D (CD), and D and E (DE). Only the loop CD has been found ordered in all three crystal structures (two structures of hIL-10 and one of vIL-10). The two other loops, AB and DE, as well as the N-terminal coil which includes the disulfide bridge Cys12–Cys108, were not seen in the electron density maps of the tetragonal hIL-10, although they were located both in the trigonal hIL-10 and in tetragonal vIL-10. For that reason, further comparison of the hIL-10 and vIL-10 structures is based on the structure of trigonal hIL-10 (Table 1). For simplicity, the hIL-10 numbering will be used also for the description of vIL-10.

### N-terminal region

As mentioned above, the most significant differences in the amino acid sequences of viral and human IL-10 are found at the N terminus (Figure 1). Because of the deletion of residues 17 to 20, Cys12 of vIL-10 is shifted by 8.8 Å toward the N terminus of helix A and is positioned in the proximity of *cis*-Pro16 of hIL-10. As a result, the disulfide bridge Cys12–Cys108 is now located 6.1 Å away from its former position, and overlaps the position of the phenyl ring of Phe15 of hIL-10 (Figure 3(a)). For these reasons, the conformation of the loop DE in the region 108 to 111 is changed to allow the formation of this disulfide bridge (Figure 3(a)), while the main-chain of residues 13 to 16 of vIL-10 makes a shortcut through the first turn of the hIL-10 helix A, accommodating *cis*-Pro16 in the position of *trans*-Pro20 of

hIL-10. The conformation of this shortcut is such that the side-chain of Phe15 (vIL-10) substitutes exactly at the position of the side-chain of Leu19 (hIL-10) in the extensive hydrophobic core of the domain. Both the N-terminal coil and the segment 108 to 110 of the loop DE are very flexible, with the temperature factors in these regions exceeding 80 Å<sup>2</sup>. This result most likely means that we were able to trace the main conformation (Figure 3(b)) of a very flexible region with partial occupancies, while some other minor conformations might not be traceable.

### Receptor binding site

The putative receptor binding site, as marked for hIL-10 (Zdanov *et al.*, 1995, 1996), includes the C terminus of helix A, loop AB, and helices B and F' (Figure 4). It consists of a hydrophobic patch formed by Leu46, Leu53, Ile145, Tyr149, and Ala152, surrounded by polar side-chains of Gln38, Asp41, Asp44, Lys49, Glu50, Lys57, Asp144, Asn148, Glu151, and Arg159. As can be seen in Figure 4, the hydrophobic patch residues, as well as a majority of polar residues, have exactly the same position and conformation in both vIL-10 and hIL-10, while the conformation of the region 39 to 45 of loop AB of vIL-10 is completely different (residues Met39, Lys40 and Asp41 are part of the helix A in the hIL-10 structure). This region appears to be as flexible as the N-terminal coil and the region 108 to 110 of loop DE. Nevertheless, the main-chain could be traced unambiguously, although only the side-chain of Thr39 was found in the electron density map. The fact that the central hydrophobic patch has exactly the same conformation might be very important, since hydrophobic interactions can account for a major part of the binding energy, as observed for the growth hormone (GH) receptor complex (de Vos *et al.*, 1992; Clackson & Wells, 1995). Taken together with the polar residues having conserved conformation, this receptor binding site appears to retain sufficient interactions to attract vIL-10

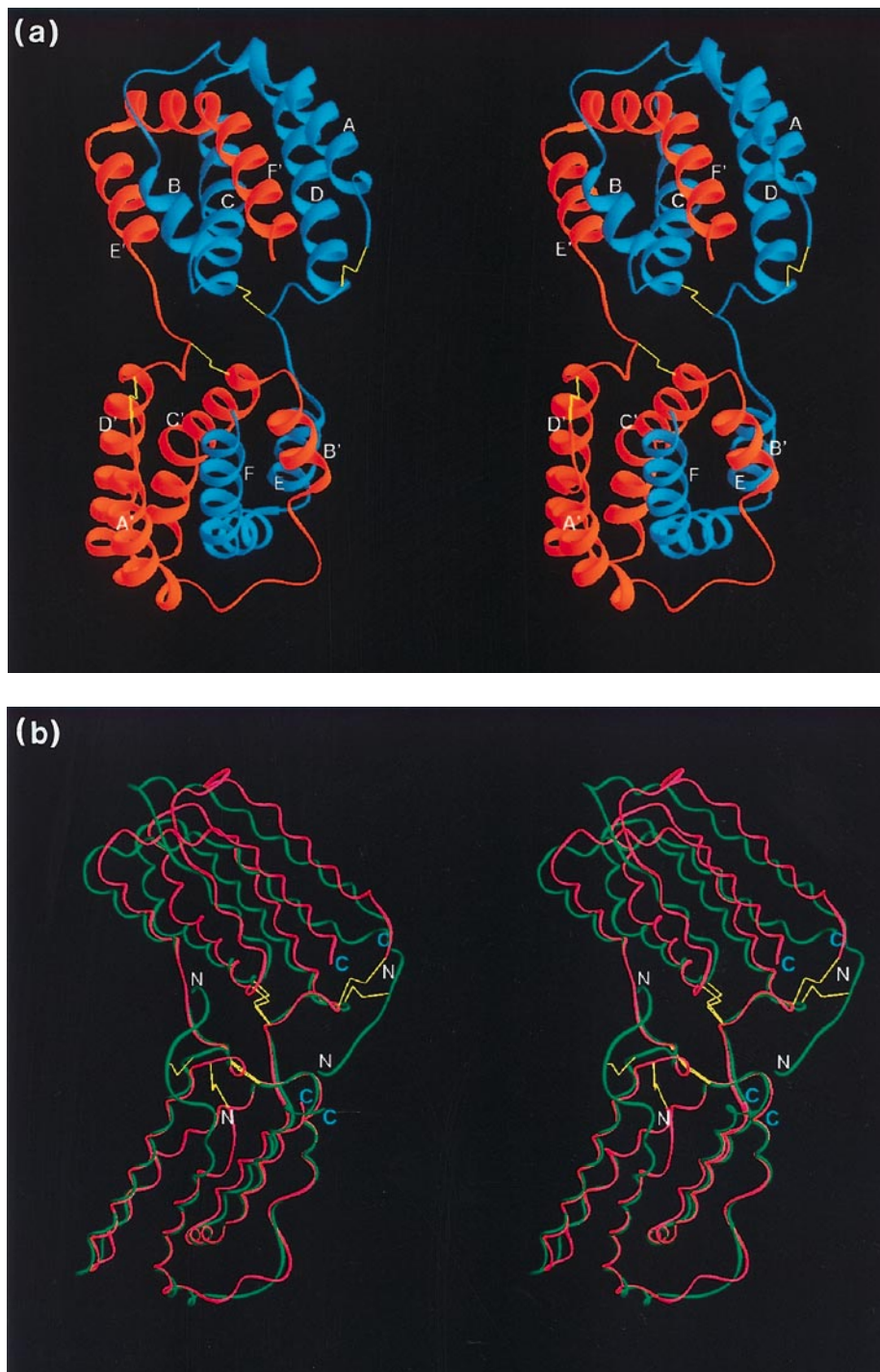


**Figure 2.** The structure of IL-10. (a) Stereo ribbon diagram of the dimer of vIL-10, with the monomers shown in red and blue and the disulfide bridges in yellow. Helices are marked as A to F for one monomer and A' to F' for the other, and they are related by a crystallographic 2-fold axis. (b) Superposition of the dimer of vIL-10 (red) with that of the hIL-10 (green). Disulfide bridges are shown in yellow. N and C termini are marked as N (white) and C (blue), respectively. The alignment of the structures is based on the superposition of the domains seen at the bottom of the Figure.

toward hIL-10R. However, due to the different conformation of the loop AB and of the lower number of interacting side-chains, the complementarity of vIL-10 toward hIL-10R appears to be not as good as for hIL-10. This conclusion agrees very well with the data on binding of vIL-10 to hIL-10R,

showing that vIL-10 has a lower specific activity (Moore *et al.*, 1993). In addition, the difference in the conformation of the loop AB may be a reason why vIL-10 does not effectively antagonize binding of hIL-10 to recombinant IL-10R (Ho & Moore, 1994; Liu *et al.*, 1997).

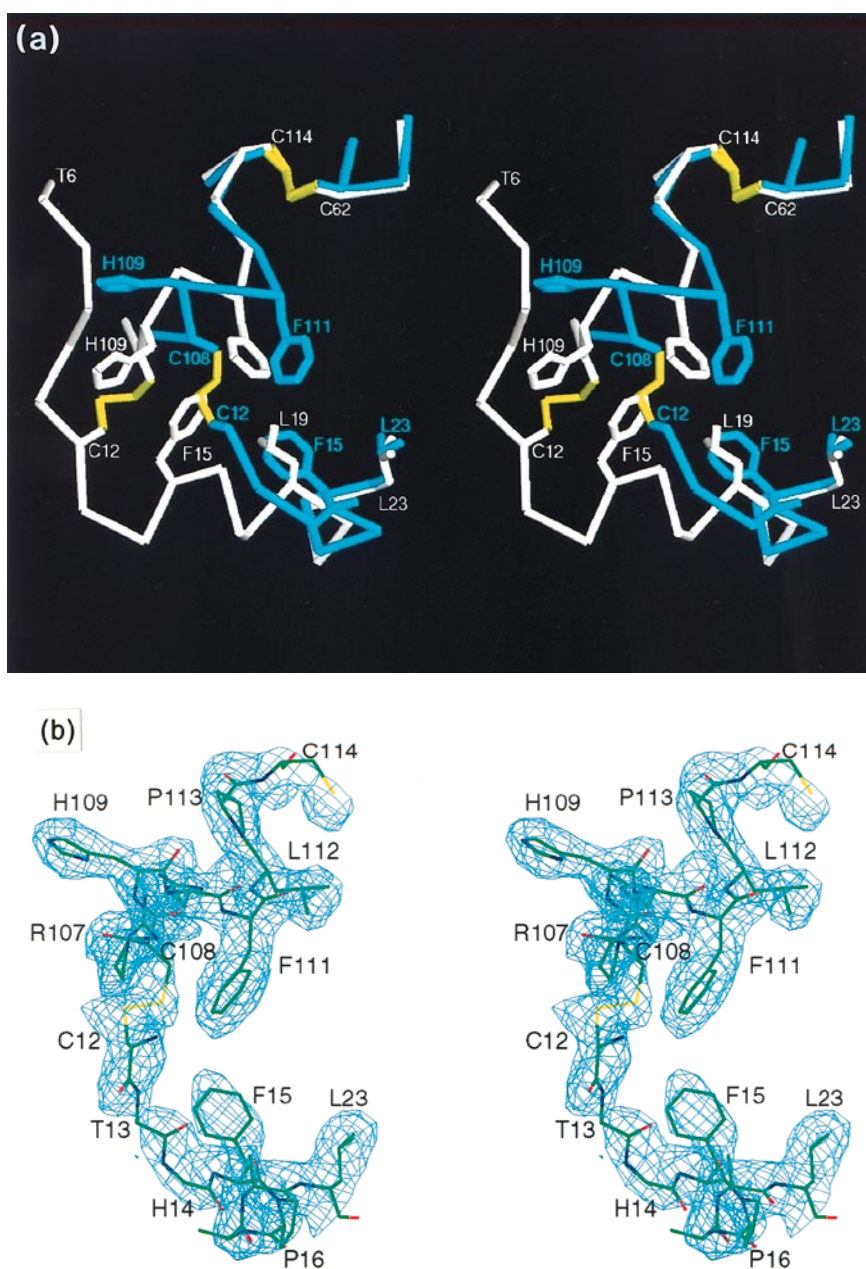


**Figure 3.** N-terminal region of vIL-10. (a) The region in the proximity of the N termini of viral (blue) and human (white) IL-10: includes N-terminal residues 12 to 23 of vIL-10, and 6 to 23 of hIL-10; residues 107 to 115 of loop DE and 60 to 63 of helix C of both vIL-10 and hIL-10. Disulfide bridges are yellow. (b) Stereo pair of an electron-density map ( $2F_o - F_c$ ) of the N-terminal coil 12 to 23 and loop 107 to 115 including very flexible regions 12 to 16 and 108 to 110. Contour level is  $0.8\sigma$ . Figure prepared with the program CHAIN (Sack, 1988).

## Discussion

Viral and cellular IL-10 share the macrophage inhibitory and B cell stimulating properties, but the ability of vIL-10 to serve as a cofactor for mast cell or  $CD4^+$  T cell stimulation is by comparison severely reduced or lacking. Moreover, the affinity of IL-10R for vIL-10 is  $\sim 1000$ -fold reduced compared to hIL-10 (Ho & Moore, 1994; Liu *et al.*, 1997). Antibodies against the known hIL-10R block biological responses to both hIL-10 and vIL-10, indicating that this receptor is required for responses to both cytokines (Liu *et al.*, 1997), but the fact that vIL-10

possesses only a subset of the functions of the hIL-10 strongly supports an idea of the existence of an accessory IL-10 receptor. It appears that the region near the N terminus of IL-10, including the N-terminal coil, helix A, and the C-terminal part of helix D, could be a good candidate for a binding site for such an accessory IL-10R subunit. If that is the case, then the completely different conformations of the N termini of vIL-10 and hIL-10 (Figures 2(b), 3(a)) will likely affect the interaction of the cytokine with this component of the IL-10 receptor system.

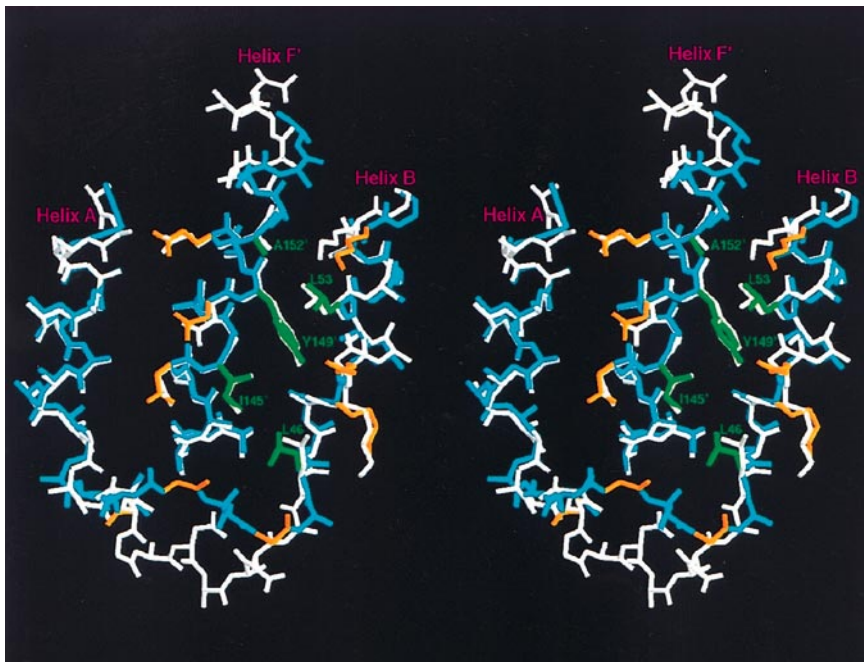


**Figure 4.** A putative receptor binding site in IL-10. Here vIL-10 is shown in blue, hIL-10 in white, the hydrophobic patch residues are in green, and polar residues in orange.

Since no data have been published on the location of the primary IL-10R binding site or on what residues are involved in its formation, we identified this site ourselves (Zdanov *et al.*, 1995), by utilizing the known crystal structure of the complex of human GH with the extracellular domain of its receptor (GHR) (de Vos *et al.*, 1992) and amino acid sequence alignment of IL-10 from various species. Subsequently, these predictions were tested after the structure of the complex of interferon  $\gamma$  (IFN $\gamma$ ) with the extracellular domain of its receptor (IFN $\gamma$ R) was published (Walter *et al.*, 1995) and the coordinates of the complex became available to us (S. Ealick, personal communication). We found that although the mutual orientation of the ligand and receptor molecules is quite different for GH/GHR and IFN $\gamma$ /IFN $\gamma$ R complexes (Walter *et al.*, 1995), the location of the primary receptor binding site on the surface of the four-helix bundle moiety and its topology are very similar (Figure 4). For such reasons, we believe that the primary receptor binding site as previously delineated by us (Zdanov *et al.*, 1995) seems to be plausible, or at least it does not contradict any currently available data.

The only component of the primary binding site which has completely different conformation in vIL-10 is the loop AB (Figure 4). We noted above that this might be the reason for the lower affinity of vIL-10 than of hIL-10 toward hIL-10R. However, we need to take into account a possibility that this might be due simply to the differences caused by crystal packing, since vIL-10 was crystallized in a tetragonal cell, while the only structure of hIL-10 in which this loop was visible was trigonal. We

found that the packing of vIL-10 dimers in the tetragonal unit cell leaves more than enough space to accommodate both the "tetragonal" and "trigonal" conformations of the loop AB, although the loop is still involved in 34 close contacts (shorter than 3.6 Å) with the symmetry-related molecules. On the other hand, in the trigonal unit cell the conformation of the loop AB is locked in place by more numerous interactions with a symmetry-related molecule (70 close contacts) and there is no room for the "tetragonal" conformation. Obviously, this means that loop AB is very flexible in solution and may change its conformation upon receptor binding. It has been shown that loop AB of unbound human IFN $\gamma$  does not have clear secondary structure (Ealick *et al.*, 1991). However, when IFN $\gamma$  binds to its receptor, the loop forms a  $3_{10}$  helical turn and changes conformation dramatically (Walter *et al.*, 1995). We assume that in the case of trigonal IL-10, the symmetry-related molecule may play a role of a surrogate receptor in the crystal, promoting "bound" or "active" conformation of the loop AB, since it resembles that of the IFN $\gamma$  bound to its receptor and it fitted perfectly the IL-10R in the computer model of hIL-10/hIL-10R complex (Zdanov *et al.*, 1996). This leads to the assumption that the conformation of this loop in vIL-10 is "inactive" and it is possible that it might become "active" only upon receptor binding. On the other hand, because of the mutations M39T, Q41E and L42V (Figure 1), this loop might never be able to assume a completely active conformation, thus affecting the binding affinity of vIL-10 toward hIL-10. The fact that this loop could not be traced in the tetragonal hIL-10, but has been traced in the

completely isomorphous crystal form of vIL-10, appears to support the idea that the conformation of the loop AB of the vIL-10 actually differs from that of hIL-10. It is obvious that these questions can be fully answered only by analyzing crystal structures of the complexes of hIL-10/hIL-10R and vIL-10/hIL-10R. This work is now in progress in our laboratory.

## Materials and Methods

The protein BCRF1 (vIL-10) used in this study was obtained by recombinant techniques, expressed in *Escherichia coli*, and purified (S. Menon, unpublished). The crystals of vIL-10 were grown by the hanging drop technique at room temperature, using 17% polyethylene glycol 4000 as precipitant, in 0.1 M sodium acetate and 0.2 M ammonium sulfate, (pH 5.6). The protein concentration was 10.0 mg/ml. The drops containing 4  $\mu$ l of protein solution and 1  $\mu$ l of well solution were equilibrated against 1 ml of well solution. Crystals appeared in two to three days and reached their maximum size (0.3 mm  $\times$  0.4 mm  $\times$  0.7 mm) in eight to ten days. They belong to the tetragonal system, space group  $P4_32_12$  with unit cell parameters  $a=b=36.27$  Å,  $c=219.60$  Å, and one monomer in the asymmetric unit. The diffraction data were collected on the RAXIS-II image plate system mounted on a Rigaku RU200 rotating anode generator, operated at 5 kW. The completeness of data at 1.9 Å resolution is 82.0% (47.0% in the 2.0 to 1.9 Å resolution shell); the  $R_{\text{merge}}$  is 8.1%. The structure was solved by the molecular replacement method with the program X-PLOR (Brunger, 1992), using as a starting model the coordinates of a single domain of the trigonal hIL-10 determined at the resolution of 1.6 Å (Table 1), and utilizing diffraction data in the 8 to 4 Å resolution shell. The best solution of the rotation function search followed by Patterson correlation refinement (Brunger, 1992) was only 1.2 times higher than the second best peak. Nevertheless, the translation function search followed by three-step rigid body refinement (in the first step the domain of IL-10 was treated as a rigid body, in the second step each helix was treated as a rigid body, and the third step was a repetition of step one) gave clear solution with the correlation value of 0.87 and an  $R$ -factor of 0.26 for the 10 to 2.5 Å resolution shell. Further refinement was carried out with programs X-PLOR (Brunger, 1992) and PROLSQ (Hendrickson, 1985; Finzel, 1987) utilizing the same set of target geometrical parameters (Engh & Huber, 1991). The structure was rebuilt using an interactive molecular graphics program FRODO (Jones, 1985). Figures 2(a), 2(b), 3(a), and 4 were prepared with the program RIBBONS (Carson, 1991).

The final model contains 142 out of 145 amino acid residues present in the expressed protein, as well as 75 water molecules. Due to their high flexibility, the side-chains of Asp13, Asn14, Gln21, Met22, Gln38, Lys40, Asp41, Glu42, Val43, Asp44, Asn45, Glu74, Lys119, Ile156, and Lys157 could not be located. The final  $R$ -factor is 0.191 for all data in the 10.0 Å to 1.9 Å resolution shell with rmsd for bonds 0.019 Å, for bond angles 0.049 Å and rmsd from planarity 0.018 Å. The average  $B$ -factors are 37.9 Å<sup>2</sup> for the main-chain atoms, 42.2 Å<sup>2</sup> for the side-chain atoms, and 40.0 Å<sup>2</sup> for all non-hydrogen atoms of vIL-10. The atomic coordinates and struc-

ture factors of vIL-10 have been deposited with the Protein Data Bank (accession numbers 1VLK and R1VLKSF, respectively).

## Acknowledgments

We thank Richard Reim, Peggy Lio and Dr Eugene Schafer of Schering-Plough Research Institute for providing us with vIL-10 producing *E. coli* cells, and Anne Arthur for editorial comments. DNAX Research Institute is funded by Schering-Plough Corporation. Research sponsored in part by the National Cancer Institute, DHHS, under contract with ABL. The contents of this publication do not necessarily reflect the views or policies of the Department of Health and Human Services, nor does mention of trade names, commercial products, or organizations imply endorsement by the U.S. Government.

## References

- Brünger, A. (1992). In *X-PLOR Version 3.1: A System for X-Ray Crystallography and NMR* Yale University Press, New Haven.
- Carson, M. (1991). RIBBONS 4.0. *J. Appl. Crystallog.* **24**, 958–961.
- Clackson, T. & Wells, J. A. (1995). A hot spot of binding energy in a hormone-receptor interface. *Science*, **267**, 383–386.
- Davies, D. R. & Chacko, S. (1993). Antibody structure. *Acc. Chem. Res.* **26**, 421–427.
- Davies, D. R. & Wlodawer, A. (1995). Cytokines and their receptor complexes. *FASEB J.* **9**, 50–56.
- de Vos, A. M., Ultsch, M. & Kossiakoff, A. A. (1992). Human growth hormone and extracellular domain of its receptor: Crystal structure of the complex. *Science*, **255**, 306–312.
- Ealick, S. E., Cook, W. J., Vijay-Kumar, S., Carson, M., Nagabhushan, T. L., Trotta, P. P. & Bugg, C. E. (1991). Three-dimensional structure of recombinant human interferon-gamma. *Science*, **252**, 698–702.
- Engh, R. & Huber, R. (1991). Accurate bond and angle parameters for X-ray protein-structure refinement. *Acta Crystallog. sect. A*, **47**, 392–400.
- Finzel, B. C. (1987). Incorporation of fast Fourier transforms to speed restrained least-squares refinement of protein structures. *J. Appl. Crystallog.* **20**, 53–55.
- Fiorentino, D. F., Bond, M. W. & Mosmann, T. R. (1989). Two types of mouse T helper cell: IV. Th2 clones secrete a factor that inhibits cytokine production by Th1 clones. *J. Expt. Med.* **170**, 2081–2095.
- Hendrickson, W. A. (1985). Stereochemically restrained refinement of macromolecular structures. *Methods Enzymol.* **115**, 252–270.
- Ho, A. S.-Y. & Moore, K. W. (1994). Interleukin-10 and its receptor. *Ther. Immunol.* **1**, 173–185.
- Ho, A. S. Y., Liu, Y., Khan, T. A., Hsu, D.-H., Bazan, J. F. & Moore, K. W. (1993). A receptor for interleukin 10 is related to interferon receptors. *Proc. Natl Acad. Sci. USA*, **90**, 11267–11271.
- Jones, T. A. (1985). Interactive computer graphics: FRODO. *Methods Enzymol.* **115**, 157–171.
- Liu, Y., Wei, S. H.-Y., Ho, A. S.-Y., Malefyt, R. W. & Moore, K. W. (1994). Expression cloning and characterization of a human IL-10 receptor. *J. Immunol.* **152**, 1821–1829.

- Liu, Y., de Waal Malefyt, R., Briere, F., Parham, C., Bridon, J. M., Banchereau, J., Moore, K. W. & Xu, J. (1997). The EBV IL-10 homolog is a selective agonist with impaired binding to the IL-10 receptor. *J. Immunol.* **158**, 605–613.
- Moore, K. W., Vieira, P., Fiorentino, D. F., Trounstein, M. L., Khan, T. A. & Mosmann, T. R. (1990). Homology of cytokine synthesis inhibitory factor (IL-10) to the Epstein Barr Virus gene BCRFI. *Science*, **248**, 1230–1234.
- Moore, K. W., O'Garra, A., de Waal Malefyt, R., Vieira, P. & Mosmann, T. R. (1993). Interleukin-10. *Annu. Rev. Immunol.* **11**, 165–190.
- Panuska, J. R., Merolla, R., Rebert, N. A., Hoffmann, S. P., Tsivitse, P., Cirino, N. M., Silverman, R. H. & Rankin, J. A. (1995). Respiratory syncytial virus induces interleukin-10 by human alveolar macrophages. Suppression of early cytokine production and implications for incomplete immunity. *J. Clin. Invest.* **96**, 2445–2453.
- Presnell, S. R. & Cohen, F. E. (1989). Topological distribution of four- $\alpha$ -helix bundles. *Proc. Natl Acad. Sci. USA*, **86**, 6592–6596.
- Rode, H. J., Janssen, W., Rosen-Wolff, A., Bugert, J. J., Thein, P., Becker, Y. & Darai, G. (1993). The genome of equine herpesvirus type 2 harbors an interleukin 10 (IL10)-like gene. *Virus Genes*, **7**, 111–116.
- Sack, J. S. (1988). CHAIN-a crystallographic modeling program. *J. Mol. Graphics*, **6**, 244–245.
- Vieira, P., Malefyt, R. W., Dang, M.-N., Johnson, K. E., Kastelein, R., Fiorentino, D. F., DeVries, J. E., Roncarolo, M.-G., Mosmann, T. R. & Moore, K. W. (1991). Isolation and expression of human cytokine synthesis inhibitory factor cDNA clones: homology to Epstein-Barr virus open reading frame BCRFI. *Proc. Natl Acad. Sci. USA*, **88**, 1172–1176.
- Walter, M. R. & Nagabhushan, T. L. (1995). Crystal structure of interleukin 10 reveals an interferon gamma-like fold. *Biochemistry*, **34**, 12118–12125.
- Walter, M. R., Windsor, W. T., Nagabhushan, T. L., Lundell, D. J., Lunn, C. A., Zauodny, P. J. & Narula, S. K. (1995). Crystal structure of a complex between interferon-gamma and its soluble high-affinity receptor. *Nature*, **376**, 230–235.
- Zdanov, A., Schalk-Hihi, C., Gustchina, A., Tsang, M., Weatherbee, J. & Wlodawer, A. (1995). Interleukin-10: crystal structure reveals the functional dimer with an unexpected topological similarity to interferon gamma. *Structure*, **3**, 591–601.
- Zdanov, A., Schalk-Hihi, C. & Wlodawer, A. (1996). Crystal structure of human interleukin-10 at 1.6 Å resolution and a model of a complex with its soluble receptor. *Protein Sci.* **5**, 1955–1962.

*Edited by R. Huber*

*(Received 6 January 1997; received in revised form 17 February 1997; accepted 20 February 1997)*